ARCHIVES OF ACOUSITCS
13, 1 2, 157 189 (1988)

HALF-PLANE EDGE AND RIGHT ANGLE WEDGE AS ELEMENTS CAUSING DIFFRACTION IN URBAN AREA

ELŻBIETA WALERIAN

Institute of Fundamental Technological Research, Polish Academy of Sciences
(00–049 Warszawa, ul. Świętokrzyska 21)

This study analyzed the acoustic fields generated by interactions between acoustic waves and the edge of a half plane and a right angle wedge. Using known solutions of the diffraction of a monochromatic wave on a half-plane and a right angle wedge, they were written in a form permitting simultaneous analysis of three wave types: plane, cylindrical and spherical. Approximate forms of solutions were adopted and the ranges of their applicability analyzed. In the space around the chosen obstacle, its efficiency was calculated with respect to a free field, for wavelengths and distances of interest in urban acoustics.

W artykule poddano analizie pola akustyczne jakie powstają na skutek oddziaływania fal akustycznych z krawędzią półpłaszczyzny i ostrzem klina o kącie rozwarcia równym kątowi prostemu. Wykorzystując znane rozwiązania dyfrakcji fali monochromatycznej na półpłaszczyźnie i ostrzu klina zapisano je w postaci pozwalającej na jednoczesną analizę trzech typów fal: fali płaskiej, cylindrycznej i kulistej. Przyjęto przybliżone postacie rozwiązań, dokonując analizy zakresu ich stosowalności. W przestrzeni wokół wybranych przeszkód obliczono ich efektywność w stosunku do pola swobodnego, dla długości fal i odległości stanowiących przedmiot zainteresowania akustyki urbanistycznej.

Basic notation

V part of the acoustic potential Ψ of the monochromatic wave dependent on the spatial coordinates: $\Psi = V\exp(-i\omega t)$,
k wave number: $k = 2\pi/\lambda = 2\pi f/c = \omega/c$, λ — wavelength, f — frequency, c — wave velocity, ω — angular frequency,
n normal to the barrier surface,
ϱ_0 radial coordinate of the source position,
ϱ radial coordinate of the position of the observation point,
ϕ_0 angular coordinate of the source position,
ϕ angular coordinate of the position of the observation point,
z_0 z-th coordinate of the source position,
z z-th coordinate of the position of the observation point.

Introduction

The notion of diffraction may be understood to mean all deviations from the laws of geometrical acoustics in the process of interactions between acoustic waves with obstacles whose acoustic properties are different from those of the ambient medium. In the simplest case, this is a step-like change in acoustic properties which occurs on the edge of a half-plane.

In practice diffraction is, e.g., a phenomenon which determines the efficiency of flat acoustic screens in the shadow area. However, the use of such screens as a measure against the noise propagation from highway requires considering changes in the acoustic field not only in the shadow area, but also throughout the space of the screen.

In general, wishing to describe the acoustic field in complex urban systems, it is first necessary to gain knowledge of the elementary processes forming the acoustic fields, including wave reflection and diffraction.

For urban systems it is acceptable to describe the acoustic field basing on the laws of geometrical acoustic, with a correction for the diffraction occurring on edges of the types of half-plane and wedge, e.g. diffraction on the half-plane type edge occurs for the flat acoustic screens mentioned above. Diffraction at the right angle wedge occurs at house corners, balconies etc. In the case of a depressed highway diffraction occurs at the wedge of the slope, this time at the wedge whose opening angle depends on the inclination angle of the slope, and which may be different from a right one.

Generally, highways can be recognized as the main noise source urban area. In the first approximation, for large distances, the highway can be considered as a source of plane waves. At shorter distances, the model of a linear source is assumed for it. Very close to the highway distinguishing individual vehicles, the waves from them are considered spherical waves. Using more complex models of highway, the acoustic field can be treated as one composed of elementary waves, e.g. plane, cylindrical and spherical.

Considering the two basic elements at which diffraction occurs (the half-plane and wedge) and three elementary wave types (plane, cylindrical and spherical), this study analyzes the acoustic fields for these cases.

Section 1 of the study presents a general description of the structure of the acoustic field for chosen cases. The starting point were the known solutions of the diffraction problem [1, 2] in which it is possible to extract the geometrical and diffraction parts. The study shows that the asymptotic forms of these solutions for the cases in question can be written in the form of the sum of waves forming independent pairs related to the real source and the image sources representing the waves reflected from the obstacle. The pair of waves related to one source consists of the geometrical wave occurring only in limited space around the barrier, and the diffraction wave present throughout the space.

The above description differs from the geometrical diffraction theory proposed

by KELLER [3, 4] in that, instead of diffraction rays describing the total effect of interaction with the obstacle, it introduces diffraction waves related to particular sources of geometrical waves. This makes it possible to explain the nature of the field at the geometrical boundaries and close to them, which cannot be done on the grounds of the geometrical diffraction theory.

Section 2 gives explicit forms of the component geometrical and diffraction waves distinguished in the description. It discusses in detail the applicability ranges of the asymptotic forms of solutions which provided the basis for the description introduced and which are different for particular cases. The regions where the conditions of asymptotic approximation are satisfied at the same time for all the cases presented coincide with the applicability range of the geometrical diffraction theory.

Taking into account the conditions met in urban area, section 3 compares the efficiency of two kinds of obstacle (half-plane and wedge) for three types of wave (plane, cylindrical and spherical) in the area of the geometrical shadow. Also, it distinguishes area where the presence of obstacle does not cause any significant disturbance and those where, as a result of interference between the waves in them, alternating increases and decreases in the total field amplitude occur.

The fields were analyzed for monochromatic waves from which complex acoustic signals are made. The description of the field used the acoustic potential which is linearly related to the acoustic pressure of the monochromatic wave.

1. Structure of the acoustic field around the half-plane and wedge

By using the appropriate approximations of the exact solutions of the problems of the wave-obstacle interactions, the acoustic potential expressions describing the total field around the obstacle can be written in the form of the sum of the geometrical and diffraction parts of the potential [1, 2].

The geometrical part of the acoustic potential can be obtained on the basis of the laws of geometrical acoustics in the form of the sum of geometrical waves coming from the real source and those from the image sources represented by the waves reflected from the obstacle surfaces.

The areas where geometrical waves are present are determined by the obstacle size. In view of this, the total geometrical field, which is the sum of geometrical waves, is discontinous. This discontinuity is compensated by the diffraction part of the acoustic potential.

After the appropriate rearrangement it was possible to represent the diffraction part of the potential in the form of the sum of diffraction waves, each related to the source of a geometrical wave. Around the geometrical boundary, where the geometrical wave from one of the sources vanishes, the related diffraction wave takes maximum values compensating the jump of the geometrical wave, providing at the same time, the continuity of the field.

On the ground of a description of the field containing the related pairs of geometrical and diffraction waves coming from the same source, one obtains a uniform description of the structure of the acoustic field around the obstacle independent of the type of wave and the kind of obstacle.

1.1. Structure of the acoustic field around the obstacle

The acoustic field of a monochromatic wave with the frequency f, around the ideal hard half-plane, can be determined by the solution of the Helmholtz equation for the acoustic potential

$$(\Delta^2 + k^2) V = 0, \tag{1}$$

with the boundary condition

$$\frac{\partial V}{\partial n} = 0. \tag{2}$$

This equation can be written in the following form:

$$V = V^g + V^d, \tag{3}$$

where V^g is the geometrical part of the acoustic potential and V^d is the diffraction part of the acoustic potential.

In a cylindrical coordinate system (Fig. 1) the equation of the half-plane

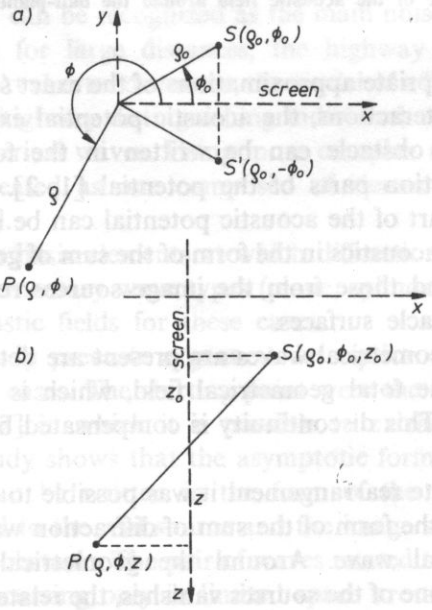

FIG. 1. The coordinate system applied: the screen is a half-plane with the equation $y = 0$, $0 \leqslant x < \infty$, or $\phi = 0$, P — observation point, S — source

disturbing the acoustic field, has the form

$$\phi = 0, \tag{4}$$

the geometrical part of the potential can be written in the form

$$V^g = \eta(\pi-\beta)\, V^i(R)+\eta(\pi-\beta')\, V^i(R'), \tag{5}$$

where

$$\beta = \phi-\phi_0, \tag{6}$$

$$\beta' = \phi+\phi_0, \tag{7}$$

$$R = R(\beta), \quad R' = R(\beta'), \tag{8}$$

R is the distance between the observation position and the source S and R' is the distance between the observation point and the image source S'.

The function $\eta(x)$ is the step function

$$\eta(x) = \begin{cases} 1, & x > 0, \\ 0, & x \leqslant 0. \end{cases} \tag{9}$$

The potential $V^i(R)$ represents a wave incident from the source S (Fig. 2), whereas the potential $V^i(R')$ represents that from the source S', namely a wave reflected from the half-plane $\phi = 0$.

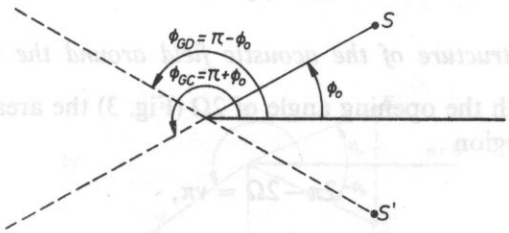

FIG. 2. The position of the shadow boundary $\phi_G = \phi_{GC} = \pi+\phi_0$ and that of the boundary of the reflected wave $\phi_G = \phi_{GD} = \pi-\phi_0$

The diffraction part of the potential can be written in the form of the sum of two diffraction waves

$$V^d = V^d[R(\beta)]+V^d[R(\beta')]. \tag{10}$$

The potential $V^d[R(\beta)]$ represents the wave generated as a result of the interaction of a wave from the source S with the edge of the half-plane, and the potential $V^d(R(\beta'))$ – the wave generated by the interaction between a reflected wave and the edge, i.e. the interaction between the wave from the image source S' and the edge.

It follows from above that each of the sources, both S and S', are sources of geometrical and diffraction waves. Geometrical waves occur only in certain areas around the half-plane, diffraction waves are present throughout the space. The direct

wave $V^i(R)$ from the source S exists in the area

$$0 < \phi < \pi + \phi_0, \tag{11}$$

where

$$\pi + \phi_0 = \phi_{GC} \tag{12}$$

is the shadow boundary (Fig. 2). The region

$$\phi_{GC} < \phi < 2\pi \tag{13}$$

is the area of the geometrical shadow where there are no geometrical waves. The reflected wave $V^i(R')$ coming from the source S' exists in the region

$$0 < \phi < \pi - \phi_0, \tag{14}$$

where

$$\pi - \phi_0 = \phi_{GD} \tag{15}$$

is the boundary of the reflected waves (Fig. 2).

In relation to the geometry of the system, the solutions obtained are symmetrized with respect to the half-plane $\phi = \pi$, hence, it is possible to limit the analysis of the field, assuming the source position to be within the interval

$$0 < \phi_0 < \pi. \tag{16}$$

1.2. Structure of the acoustic field around the wedge

For a wedge with the opening angle of 2Ω (Fig. 3) the area of the acoustic field description is the region

$$2\pi - 2\Omega = \nu\pi, \tag{17}$$

where

$$\nu > 1, \tag{18}$$

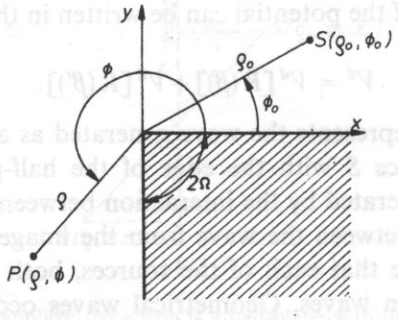

FIG. 3. The position of the right angle wedge in the coordinate system applied

i.e. the region outside the wedge. For wedges for which the parameter ν satisfies condition (18), the formulae given below are valid if the appropriate value of ν is put in plane of $\nu = 3/2$ represented a right angle wedge.

The acoustic field which would emerge as a result of the interaction between the acoustic wave and the ideal rigid right angle wedge, is described by the acoustic potential satisfying the Helmholtz equation (1), with the boundary conditions (2), which in this case must be satisfied on two half-planes forming the wedge (Fig. 3).

Just as for a single half-plance, this potential can be written in the form of sum (3) of the geometrical part V^g and the diffraction part V^d of the potential. The geometrical part V^g (Fig. 4) consists of three waves: the wave ($V^i(R)$) coming from the real source S, the wave ($V^i(R')$) reflected from the half-plane $\phi = 0$, coming from the source S', and the wave ($V^i(R'')$) reflected from the half-plane $\phi = 3\pi/2$ coming from

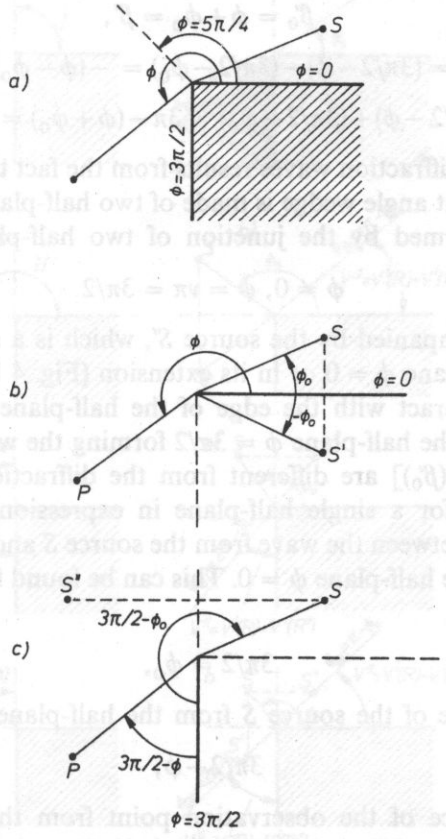

FIG. 4. The sources of the waves making up the acoustic field around the right angle wedge: a) the half-planes $\phi = 0$ and $\phi = 3\pi/2$ making up the wedge; b) the position of the source S' representing the wave $V^i(R')$ reflected from the half-plane $\phi = 0$; c) the position of the source S'' representing the wave $V^i(R'')$ reflected from the half-plane $\phi = 3\pi/2$

the source S''

$$V^g = \eta(\pi-\beta)\eta(3\pi/2-\phi)V^i(R)+\eta(\pi-\beta')\eta(3\pi/2-\phi)V^i(R') + \eta(\pi-\beta'')\eta(3\pi/2-\phi)V^i(R''), \quad (19)$$

$$\beta = \phi-\phi_0, \quad (20)$$

$$\beta' = \phi+\phi_0, \quad (21)$$

$$\beta'' = (3\pi/2-\phi)+(3\pi/2-\phi_0) = 3\pi-(\phi+\phi_0), \quad (22)$$

$$R = R(\beta), \quad R' = R(\beta'), \quad R'' = R(\beta''). \quad (23)$$

The diffraction part of the potential is the sum of the four waves

$$V^d = V^d[R(\beta_0)+V^d[R(\beta'_0)]+V^d[R(\beta_{3\pi/2})]+V^d[R(\beta'_{3\pi/2})], \quad (24)$$

$$\beta_0 = \phi-\phi_0 = \beta, \quad (25)$$

$$\beta'_0 = \phi+\phi_0 = \beta', \quad (26)$$

$$\beta_{3\pi/2} = (3\pi/2-\phi)-(3\pi/2-\phi_0) = -(\phi-\phi_0) = -\beta, \quad (27)$$

$$\beta'_{3\pi/2} = (3\pi/2-\phi)+(3\pi/2-\phi_0) = 3\pi-(\phi+\phi_0) = 3\pi-\beta' = \beta''. \quad (28)$$

The existence of four diffraction waves results from the fact that the wedge is made of two half-planes. A right angle wedge is made of two half-planes. A right angle can be recognized as one formed by the junction of two half-planes (Fig. 4):

$$\phi = 0, \phi = \nu\pi = 3\pi/2. \quad (29)$$

The source S is accompanied by the source S', which is a specular reflection of the source S in the half-plane $\phi = 0$ or in its extension (Fig. 4 b). The waves from these two sources S, S' interact with the edge of the half-plane $\phi = 0$. This interaction occurs in presence of the half-plane $\phi = 3\pi/2$ forming the wedge therefore the waves $V^d[R(\beta_0)]$ and $V^d[R(\beta'_0)]$ are different from the diffraction waves $V^d[R(\beta)]$ and $V^d[R(\beta')]$ occurring for a single half-plane in expression (10).

The interaction between the wave from the source S and the half-plane $\phi = 3\pi/2$ is similar to that of the half-plane $\phi = 0$. This can be found from expressions (27) and (28), where:

$$3\pi/2 = \phi_0, \quad (30)$$

is the angular distance of the source S from the half-plane $\phi = 3\pi/2$ (Fig. 4c), and

$$3\pi/2-\phi, \quad (31)$$

is the angular distance of the observation point from this plane.

Thus, in analogy to (25) and (26) for the half-plane $\phi = 0$, expressions (27) and (28) are the difference and the sum of the angular distances of the source and observation point from the half-plane $\phi = 3\pi/2$.

As a result of a specular reflection of the real source S in the half-plane $\phi = 3\pi/2$

there occurs the source S'' (this reflection may occur in the half-plane $\phi = 3\pi/2$ or its extension). The result of the interaction between the wave from the source S and the half-plane edge $\phi = 3\pi/2$ in the presence of the half plane $\phi = 0$ is the diffraction wave $V^d\,[R(\beta_{3\pi/2})]$. All the four diffraction waves (24) occur throughout the space around the wedge, on the other hand, geometrical waves only do so in certain areas determined by the source position ϕ_0. For this reason, it is convenient to distinguish four regions of the source position (Fig. 5).

If the source is in region I (Fig. 5 (I))

$$0 < \phi_0 < \pi/2, \tag{32}$$

the direct wave $V^i(R)$ occurs in the region

$$0 < \phi < \pi + \phi_0, \tag{33}$$

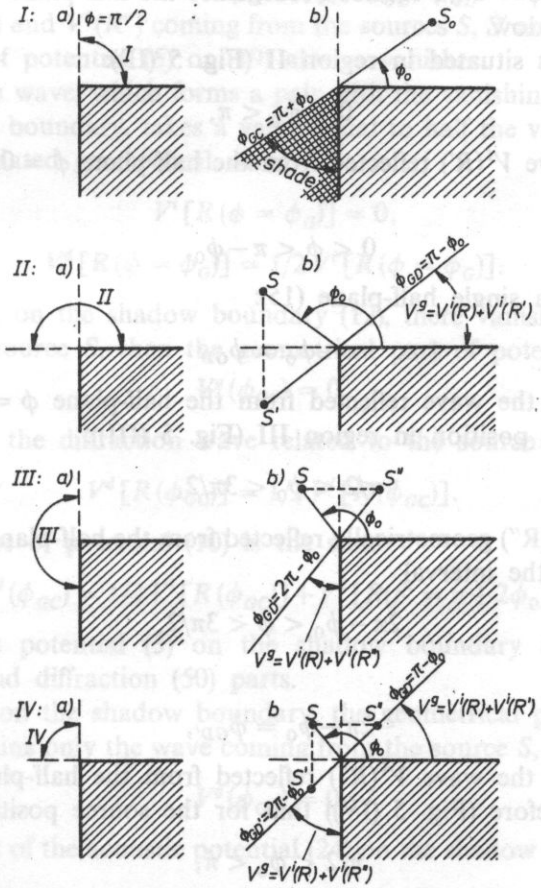

FIG. 5. The four regions of the source position distinguished here: I – $(0 < \phi_0 < \pi/2)$, II – $(0 < \phi_0 < \pi)$, III – $(\pi/2 = \phi_0 < 3\pi/2)$, IV – $(\pi/2 < \phi_0 < \pi)$. *a*) the region of the real source position, *b*) region of an image sources position corresponding to the position of a given real source and areas where particular geometrical waves occur

where, just as for a single half-plane (12)

$$\pi+\phi_0=\phi_{GC}, \tag{34}$$

is the shadow boundary. In the space

$$\phi_{GC}<\phi<3\pi/2 \tag{35}$$

the geometrical shadow occurs, where there are no geometrical waves. For the right angle wedge, this area is smaller than that for a single half-plane, since the part of the space

$$3\pi/2<\phi<2\pi \tag{36}$$

is occupied by the wedge itself.

If the source is situated in region I (32), the wave $V^i(R'')$ geometrically reflected from the half-plane $\phi=3\pi/2$ cannot occur, since the half-plane $\phi=3\pi/2$ is within the geometrical shadow.

If the source is situated in region II (Fig. 5 (II)):

$$0<\phi_0<\pi, \tag{37}$$

then occurs the wave $V^i(R')$ reflected from the half-plane $\phi=0$. It appears in the interval

$$0<\phi<\pi-\phi_0, \tag{38}$$

where, just as for a single half-plane (15):

$$\pi-\phi_0=\phi_{GD} \tag{39}$$

is the boundary of the wave reflected from the half-plane $\phi=0$.

For the source position in region III (Fig. 5 (III)):

$$\pi/2<\phi_0<3\pi/2, \tag{40}$$

there is the wave $V^i(R'')$ geometrically reflected from the half-plane $\phi=3\pi/2$, and its occurrence area is the interval

$$2\pi-\phi_0<\phi<3\pi/2, \tag{41}$$

where

$$2\pi-\phi_0=\phi_{GD'}, \tag{42}$$

is the boundary of the wave $V^i(R'')$ reflected from the half-plane $\phi=3\pi/2$.

It follows therefore (Fig. 5 (IV)) that for the source position in region IV:

$$\pi/2<\phi_0<\pi, \tag{43}$$

in the space around the wedge there is no shadow area, but there are two reflected waves: the wave $V^i(R')$ reflected from the half-plane $\phi=0$ (in region (38)) and the wave $V^i(R'')$ reflected from the half-plane $\phi=3\pi/2$ (in region (41)).

In view of the geometry of the system, the descriptions of the acoustic field are symmetrical with respect to the half-plane $\phi = 5\pi/4$ (Fig. 4a). Therefore, the complete analysis of the field requires to consider the source position only in the interval

$$0 < \phi_0 < 5\pi/4. \tag{45}$$

1.3. Acoustic field on geometrical boundaries

In the assumed coordinate system, the geometrical boundaries are half-planes with equations $\phi = \text{const}$. They are the boundary ϕ_{GC} of the shadow (12), (34) the boundary ϕ_{GD} of the wave reflected from the half-plane $\phi = 0$ (15), (39), and, in addition, for the wedge, the boundary ϕ_{GD} of the wave reflected from the half-plane $\phi = 3\pi/2$ (42).

On the geometrical boundaries $\phi_G = \phi_{GC}$, ϕ_{GD}, $\phi_{GD'}$ one of the geometrical waves $V^i(R)$, $V^i(R')$ and $V^i(R'')$ coming from the sources S, S' and S'' making up the geometrical part of potential (5) or (19) always vanishes.

The diffraction wave, which forms a pair with the vanishing geometrical wave, on the geometrical boundary, takes a value equal to half the value of the acoustic potential of the related geometrical wave,

$$V^i[R(\phi = \phi_G)] = 0, \tag{46}$$

$$V^d[R(\phi = \phi_G)] = 1/2\, V^i[R(\phi = \phi_G)]. \tag{47}$$

For the half-plane, on the shadow boundary (12), there vanishes the wave $V^i(R)$ coming from the source S, then the geometrical part of potential (5) becomes

$$V^g(\phi_{GC}) = 0. \tag{48}$$

At the same time, the diffraction wave related to the source S, takes the form

$$V^d[R(\phi_{GC})] = 1/2\, V^i[R(\phi_{GC})]. \tag{49}$$

The diffraction part of potential (10) is the sum

$$V^d(\phi_{GC}) = 1/2\, V^i[R(\phi_{GC})] + V^d[R(\beta' = \pi + 2\phi_0)]. \tag{50}$$

The total acoustic potential (3) on the shadow boundary is the sum of the geometrical (48) and diffraction (50) parts.

For a wedge, on the shadow boundary, the geometrical part of the acoustic potential (19) contains only the wave coming from the source S, which vanishes, i.e.

$$V^g(\phi_{GC}) = 0. \tag{51}$$

The diffraction part of the acoustic potential (24) on the shadow boundary takes the form

$$V^d(\phi_{GD}) = 1/2\, V^i[R(\phi_{GC})] + V^d[R(\beta'_0 = \pi + 2\phi_0)] + V^d[R(\beta_{3\pi/2} = -\pi)] + V^d[R(\beta'_{3\pi/2} = 2\pi - 2\phi_0)] \tag{52}$$

Just as for a single half-plane, the total acoustic potential on the shadow boundary consists only of the diffraction part (52).

For the case of a single half-plane on the boundary of the wave $V^i(R')$ reflected from the half-plane $\phi = 0$, the geometrical part of potential (5) takes the form:

$$V^g(\phi_{GD}) = V^i(R(\phi_{GD})]. \tag{53}$$

In turn, the diffraction part of potential (10) takes the form

$$V^d(\phi_{GD}) = V^d[R(\beta = \pi - 2\phi_0)] + 1/2\, V^i[R'(\phi_{GD})]. \tag{54}$$

The total acoustic potential on the boundary of the reflected wave is the sum of potentials (53) and (54).

For the case of a wedge on the boundary of the wave $V^i(R')$ reflected from the half-plane $\phi = 0$, the geometrical part of potential (19) takes the form of (53). In turn the expression of the diffraction part (24) is as follows:

$$V^d(\phi_{GD}) = V^d[R(\beta_0 = \pi - 2\phi_0)] + 1/2\, V^i[R'(\phi_{GD})] + V^d[R(\beta_{3\pi/2} = 2\phi_0 - \pi)] + V^d[R(\beta'_{3\pi/2} = 2\pi)]. \tag{55}$$

The total potential is the sum of potentials (53) and (55).

In addition, in the case of a wedge, there can occur the boundary (42) of the wave $V^i(R'')$ reflected from the half-plane $\phi = 3\pi/2$. The geometrical potential (19) takes the form

$$V^g(\phi_{GD'}) = V^i(R(\phi_{GD'})], \tag{56}$$

and the diffraction part (24) of the potential becomes

$$V^d(\phi_{GD'}) = V^d[R(\beta_0 = 2\pi - 2\phi_0)] + V^d[R(\beta'_0 = 2\pi)] + V^d[R(\beta_{3\pi/2} = 2\phi_0 - \pi)] + 1/2\, V^i[R''(\phi_{GD'})]. \tag{57}$$

The total field is the sum of potentials (56) and (57).

2. Explicit forms of acoustic potentials describing the acoustic field around the half-plane and right angle wedge for plane, cylindrical and spherical waves

The first step towards the description of the acoustic field shown in Sect. 1 is the division of the expression describing the potential into the geometrical and diffraction parts (3).

The division of an exact solution describing the acoustic potential around the half-plane into the geometrical (5) and diffraction (10) parts is only possible for the incident plane wave. In the case of cylindrical and spherical waves, this division can be peformed only for the approximate form of solution which is obtained as the condition is satisfied [2]

$$kR_1 \gg 1, \tag{58}$$

where R_1 is the shortest distance between the source and the observation point calculated through the edge.

R_1 can be treated as the parameter which takes a form which depends on the wave type. Considering the fact that the plane wave is the limiting case of a wave radiated by the source which is in infinity, in the assumed coordinate system the distance R_1 is

– for the plane wave

$$R_1 = \varrho, \tag{59}$$

– for the cylindrical wave

$$R_1 = \varrho_0 + \varrho, \tag{60}$$

– for the spherical wave

$$R_1 = [(\varrho_0+\varrho)^2+(z-z_0)^2]^{1/2}. \tag{61}$$

According to expressions (58) and (60), for the cylindrical wave, the division of the potential into the geometrical and diffraction parts is possible in the case of system in which the source or the observation point are far from the diffraction edge (with respect to the wavelength). For the spherical wave, according to expressions (58) and (61), it is possible, just as for the cylindrical wave, when the source or the observation point are far from the edge and also when the source and the observation point are distant enough along the z-axis ($k|z-z_0| \gg 1$).

In the case of interaction between the waves and the wedge the division of the acoustic potential into the geometrical (19) and diffraction (24) parts can be only made when the approximate form of an exact solution is used. The approximation conditions are following:

– for the plane wave

$$k\varrho \gg 1, \tag{62}$$

– for cylindrical and spherical waves

$$\frac{k\varrho_0\varrho}{R_1} \gg 1. \tag{63}$$

Since the source of the plane wave is in infinity, it can be said, in general, that if there is the interaction between three types of wave plane, cylindrical and spherical, and the wedge, the potential can be divided into the geometrical and diffraction parts only if the source and the observation point are at the same time far from the wedge.

It follows from the above that for all the six cases considered (two kinds of obstacle half-plane and wedge, for which each time there is the diffraction of three wave types plane, cylindrical and spherical) the common area where solutions can be divided into the geometrical and diffraction parts is the area which lies far from the diffraction edge. It would be applied only to systems in which the source is also far enough from the edge.

To move over from the symbolic-qualitative description of the acoustic field to

a quantitative one, we need to know explicit forms of functions describing the components of the geometrical parts of the potential (5), (19) and the diffraction parts (10), (24).

The geometrical parts of potentials are made up of waves radiated by sources whose positions are only different in the angular coordinate. Thus the distance $R(\alpha)$ between observation point and the particular source differs only in an angle α. Therefore, for every type of wave: plane, cylindrical, spherical propagation from these sources can be described by the same expression where the right quantity $R(\alpha)$ must be put. This will be presented in Sect. 2.1.

Then step leading to the description given in Sect. 1 is the analysis of simplified expressions describing the components of the diffraction part of the potentials. These simplified expressions are valid in areas appropriately distant from the geometrical boundaries tied up to successive sources. Moreover, it is possible to describe the diffraction, waves on the geometrical boundaries by means of simple expressions.

In the case of not too large area in which simplified expressions for diffraction waves are not valid on the basis of the field continuity, principle the field in this area can be determined by extrapolation from the value taken in the area where approximation is valid up to the value taken on the boundary itself. In this way, one obtains a description of the field throughout the space around the barrier.

The appropriate explicit forms of functions describing the diffraction waves in areas far from the geometrical boundaries and on the various boundaries are shown in points 2.2 and 2.3.

The applicability range of the description presented and its accuracy are discussed in subsection 2.4.

2.1. Explicit forms of the geometrical part of the acoustic potential

In the expression for the geometrical part of the potential for the half-plane (5) it is necessary to substitute the explicit forms of functions describing the waves

$$V^i(R(\alpha)], \tag{64}$$

where

$$\alpha = \beta, \beta'. \tag{65}$$

$R(\alpha)$ is successively the distance of the observation point from the sources S and S'. In the expression for the geometrical part of the potential for the wedge (19) it is necessary to substitute the explicity forms of function (64) for

$$\alpha = \beta, \beta', \beta''. \tag{66}$$

where $R(\alpha)$ is, successively, the distance of the observation point from the sources S, S' and S''.

The explicit forms of function (64) for chosen types of wave, in the assumed coordinate system, are as follows

– for a plane wave:

$$V^i[R(\alpha)] = \exp[ikR(\alpha)], \tag{67}$$

$$R(\alpha) = -\varrho\cos\alpha, \tag{68}$$

– for a cylindrical wave:

$$V^i[R(\alpha)] = \sqrt{\frac{2}{kR(\alpha)}}\exp\{i[kR(\alpha)-\pi/4\}, \tag{69}$$

$$R(\alpha) = [\varrho_0^2+\varrho^2-2\varrho_0\varrho\cos\alpha]^{1/2}, \tag{70}$$

– for a spherical wave:

$$V^i[R(\alpha)] = \frac{\exp[ikR(\alpha)]}{kR(\alpha)}, \tag{71}$$

$$R(\alpha) = [\varrho_0^2+\varrho^2-2\varrho_0\varrho\cos\alpha+(z-z_0)^2]^{1/2}. \tag{72}$$

2.2 Explicit forms of the diffraction part of the acoustic potential

From well-known expressions [1, 2] for the diffraction part of the acoustic potential for chosen kinds of obstacles (a half-plane and right-angle wedge) and three types of waves plane, cylindrical and spherical, the diffraction waves related to sources distant by $R(\alpha)$ from the observation point can be represented in the form

$$V^d[R(\alpha)] = P(\alpha,\nu)\frac{\exp[i\{k[R_1-R(\alpha)]+\pi/4\}]}{\sqrt{2\pi k\varrho}}\times d[R(\alpha)]\,V^i[R(\alpha)], \tag{73}$$

$$P(\alpha,\nu) = \frac{1}{2\nu}\sin(\pi/\nu)\frac{1}{\cos(\pi/\nu)-\cos(\alpha/\nu)}. \tag{74}$$

where $d[R(\alpha)]$ is a coefficient depending on the type of the wave. Formulae (73) and (74) are valid if conditions (58), (62) and (63), and the inequality

$$k[R_1-R(\alpha)] \gg 1. \tag{75}$$

are satisfied. Condition (75) means that the observation point must be far from the geometrical boundaries: the shadow boundary ϕ_{GC} (12), (34), the boundary ϕ_{GD} of the wave reflected from the half-plane $\phi = 0$ (15), (39), and the boundary $\phi_{GD'}$, of the wave reflected from the half-plane $\phi = 3\pi/2$ (42).

Expressions (73) and (74) are valid for wedges with an opening angle satisfying condition (18). A single half-plane is a special case of a wedge with the opening angle

$$2\Omega = 0. \tag{76}$$

Hence, from expressions (17), for the half-plane

$$\nu = 2. \tag{77}$$

In the case of the half-plane, expression (73) must be applied to determine the two

diffraction waves $V^d[R(\alpha)]$ which are part of the diffraction part of potential (10) for

$$\alpha = \beta, \beta'. \tag{78}$$

Then the diffraction part of the acoustic potential can be rewritten in relation to the incident wave $V^i(R)$ coming from the real source S:

$$V^d = P(\phi, \phi_o, \nu = 2)\frac{\exp\{i[k(R_1 - R) + \pi/4]\}}{\sqrt{2\pi k\varrho}} d(R)\, V^i(R), \tag{79}$$

$$P(\phi, \phi_0, \nu = 2) = -\frac{1}{2}\left[\frac{1}{\cos\dfrac{\phi - \phi_0}{2}} + \frac{1}{\cos\dfrac{\phi + \phi_0}{2}}\right]. \tag{80}$$

Depending on the incident wave type, the coefficient $d(R)$ takes the forms:

– for a plane wave

$$d(R) = 1, \tag{81}$$

– for a cylindrical wave

$$d(R) = \sqrt{\frac{R}{\varrho_0}}, \tag{82}$$

– for a spherical wave:

$$d(R) = \frac{R}{\sqrt{R_1 \varrho_0}}. \tag{83}$$

From formulae (59), (67), (68) and (81) the explicit form of the diffraction part of the acoustic potential for a plane wave is as follows:

$$V^d = P(\phi, \phi_0, \nu = 2)\frac{\exp[i(k\varrho + \pi/4)]}{\sqrt{2\pi k\varrho}}. \tag{84}$$

Hence, it follows that the diffraction part of the acoustic potential for a plane wave interacting with half-plane can be regarded as a wave of a cylindrical type generated by the edge. The amplitude of this wave decreases as a root of the distance from the edge ϱ. It differs from the cylindrical wave only by the directional coefficient $P(\phi, \phi_0, \nu = 2)$. In a superposition with the geometrical part of the acoustic potential (5), this wave gives the total acoustic field which appears as a result of the interaction between the plane wave and the half-plane.

On the ground of the reciprocity theorem it is possible to interchange the source and the observation point positions. Thus, for cylindrical and spherical waves, according to (58) it can be set that it is the source which is far from the edge. Then the coefficients $d(R)$, (82) and (83), can be interpreted as measures of the relative curvature of the wave fronts interacting with the edge. The emerging diffraction

waves are cylindrical-type waves deformed by the coefficient $d(R)$, with the directional coefficients $P(\phi, \phi_0, \nu = 2)$ (80), generated by the diffraction edge.

For the wedge, the diffraction part of the acoustic potential (24) contains four diffraction waves $V^d[R(\alpha)]$. To calculate them, it is necessary to use expression (73) for

$$\alpha = \beta_0, \beta'_0, \beta_{3\pi/2}, \beta'_{3\pi/2}. \tag{85}$$

Moreover, inequality (75) must be satisfied for all $R(\alpha)$.

Using the relations between the angle α occurring for the wedge, (25)–(28), the diffraction part of the acoustic potential (24) can be rewritten in relation to the wave $V^i(R)$ coming from the real source S:

$$V^d = P(\phi, \phi_0, \nu = 3/2) \frac{\exp\{i[k(R_1 - R) + \pi/4]\}}{\sqrt{2\pi k\varrho}} d(R)\, V^i(R), \tag{86}$$

$$P(\phi, \phi_0, \nu = 3/2) = \frac{2}{3}\sin(2\pi/3) \left[\frac{1}{\cos\frac{2\pi}{3} - \cos\frac{2(\phi - \phi_0)}{3}} + \frac{1}{\cos\frac{2\pi}{3} - \cos\frac{2(\phi + \phi_0)}{3}} \right]. \tag{87}$$

It follows hence that if the waves of the three chosen types interact with the wedge, the diffraction part of the acoustic potential (86) differs from the diffraction part for half-plane (79) just in the directional coefficient $P(\phi, \phi_0, \nu)$. For the half-plane it has the form of (80), for the wedge that of (87). The other conclusions concerned with the interpretation of the diffraction part of the acoustic potential remain valid. For the six analyzed cases of wave interaction with obstacles the fulfilling of conditions (58), (62), (63) and (75) gives the diffraction part of acoustical potential the same as that derived on the ground of geometrical diffraction theory.

2.3. Explicit forms of the acoustic potential on geometric boundaries

The geometrical parts of the acoustic potential $V^g(\phi_G)$ on the geometrical boundaries for the three chosen types of waves and two kinds of obstacles can be obtained by substituting the appropriate forms of geometrical waves (64) in expressions (48), (51), (53) and (56).

In the expressions describing the diffraction parts of the acoustic potential $V^d(\phi_G)$ on the geometrical boundaries, one of the components of the diffraction waves is always determined by the explicit form of the potential of the geometrical wave which vanishes on a given boundary (46), (47). If condition (75) is satisfied, the other diffraction waves occurring in expressions (50) and (54) can be determined from formula (73).

E.g. on the shadow-boundary, for the half-plane the total acoustic potential is equal to the diffraction part $V^d(\phi_{GD})$ (50). In expression (50), the first term is obtained, depending on the wave type, from one of expressions (67)–(72). In turn, the other term can be determined from (73) only if inequality (75) is satisfied for it.

In the case of the wedge, in expressions (52), (55) and (57) describing the diffraction parts of the potential on the geometrical boundaries, there are components related to the vanishing geometrical wave (40), (47) and those which, after satisfying condition (75), can be determined by expression (73). Moreover, there are also terms of the form

$$V^d[R(\alpha = n\pi, \nu)], \tag{88}$$

$$n = 0, \pm 1, \pm 2, \ldots, \tag{89}$$

which cannot be described by means of expressions (73) and (74) because the singularity occurs in expression (74) for $\alpha = n\pi$. In this case, the directional coefficients in the form

$$P(\alpha = n\pi, \nu), \tag{90}$$

should be replaced by their boundary values which can be obtained from the exact solution of the Helmholtz equation for required boundary conditions [1]

$$P(\alpha = n\pi, \nu) = -(1/2\nu)\operatorname{ctg}(\pi/\nu). \tag{91}$$

For the half-plane:

$$P(\alpha = n\pi, \nu = 2) = 0 \tag{92}$$

i.e., according to expression (50), this problem does not exist. In turn for the right angle wedge,

$$P(\alpha = n\pi, \nu = 3/2) = -(1/3)\operatorname{ctg}(2\pi/3). \tag{93}$$

This makes possible to use formula (52), (55) and (57) for determining the diffraction parts of the potential $V^d(\phi_G)$ on the geometrical boundaries wherever condition (75) is satisfied for components of diffraction waves without singularities.

2.4. Accuracy of the approximate formulae applied – ranges of applicability

The division of an exact solution describing the acoustic potential around the half-plane into the geometrical and diffraction part is only possible for the incident plane wave [2]. The geometrical part of the potential is described by expansion (5). In turn, the diffraction part in the exact solution consists of two diffraction waves, which, in keeping with the notation adapted here, have the form

$$V^d[R(\alpha)] = -\operatorname{sgn}(\pi - \alpha) f(w)\, a[R_1, R(\alpha)]\, V^i[R(\alpha)], \tag{94}$$

where for the plane wave interacting with the half-plane

$$\alpha = \beta, \beta', \tag{95}$$

$$a[R_1, R(\alpha)] = 1/2. \tag{96}$$

The function

$$f(w) = \frac{F(w)}{F(0)}, \tag{97}$$

represents the reduced Fresnel integral

$$F(w) = \int_{w}^{\infty} \exp(i\mu^2)\, d\mu, \tag{98}$$

where

$$w = \sqrt{k[R_1 - R(\alpha)]}, \tag{99}$$

is the square root, calculated in wavelengths, of the difference in the paths passed by the waves to the observation point directly from the source ($R(\alpha)$) and through the edge (R_1).

For the cylindrical and spherical waves interacting with the half-plane, the solution in the form of the sum of the geometrical part of the acoustic potential (5) and the diffraction part (10) whose component diffraction waves are given by expression (94) is the approximate form of the solution which is valid if condition (58) is satisfied.

– for cylindrical wave:

$$a[R_1, R(\alpha)] = \sqrt{\frac{R(\alpha)}{2[R_1 + R(\alpha)]}}, \tag{100}$$

– for spherical wave

$$a[R_1, R(\alpha)] = \sqrt{\frac{R^2(\alpha)}{2R_1[R_1 + R(\alpha)]}}. \tag{101}$$

On the geometrical boundaries (12) and (15) $\phi_G = \phi_{GC}, \phi_{GD}$ for diffraction waves related to the vanishing geometrical waves for all the three types of waves, one obtains the equalities:

$$R(\phi = \phi_G) = R_1, w[R_1, R(\phi = \phi_G)] = 0. \tag{102}$$

Hence, after substituting expressions (102) successively in formulae (100), (97) and (94) it can be seen that equality (47) is valid on the geometrical boundaries.

If condition (75) is satisfied,

$$w[R_1, R(\alpha)] = \sqrt{k[R_1 - R(\alpha)]} \gg 1, \tag{103}$$

the reduced Fresnel integral (97) can be replaced by the first term of a series expansion:

$$f(w) = \frac{\exp[i(w + \pi/4)]}{\sqrt{\pi}\, w}\left[1 + \sum_{n=1}^{\infty} \frac{\prod_{j=1}^{n}(2j-1)}{(2iw^2)^n}\right]. \tag{104}$$

Then, the expression for the diffraction part of the acoustic potential is obtained in the form of (79). This can be done for

$$|w| \geqslant 3 \tag{105}$$

when the error is of the order of the absolute value of the first omitted term, i.e. $(2\sqrt{\pi}\, w^3)^{-1} \sim 0.01$.

For a plane wave interacting with a half-plane, the angular width Δ can be determined for the regions around the geometrical boundaries ϕ_G for $|w| = 3$ inside which expression (79) is not valid

$$\phi_G - \Delta < \phi < \phi_G + \Delta, \tag{106}$$

$$\Delta = 2\arcsin\left(\sqrt{\frac{4.5}{k\varrho}}\right), \tag{107}$$

$$k\varrho \geqslant 4.5. \tag{108}$$

For cylindrical and spherical waves, if condition (58) is initially satisfied, the angular width Δ of the regions around the geometrical boundaries (for $|w| = 3$) where formula (79) is not valid, is

$$\Delta = 2\arcsin\left(\sqrt{\frac{4.5\,(kR_1 - 4.5}{k\varrho_0 k\varrho}}\right), \tag{109}$$

$$kR_1 \geqslant 4.5. \tag{110}$$

For plane and cylindrical waves, and also a spherical one (for $z = z_0$), Table 1 shows the angular widths Δ of the regions, around the geometrical boundaries, inside which expression (79) cannot be applied for preset parameters $k\varrho$ and $k\varrho_0$. Also, Table 1 shows the approximate values of the absolute distances of the observation point and the source from the edge for two chosen frequencies $f = 500$ and 1000 Hz as typical of noise in urban area.

It can be said in general (Table 1) that for decreasing values of the parameters $k\varrho$ and $k\varrho_0$, the region in which the approximate expression (79) is valid becomes narrower. Thus for small parameters $k\varrho$ and $k\varrho_0$ effective use of the approximate expressions is impossible.

In the case of the wedge, for the exact solution to be divided into the geometrical and diffraction parts, assumptions (62) and (63) must be satisfied. At the same time if condition (75) is fulfilled the diffraction waves can be described by formula (73). It is more difficult to determine the angular width of the regions where these conditions are not met as in the case of a single half-plane. On the other hand, it is possible to estimate them as being of the same order as those in the case of interaction between the chosen wave types and the half-plane.

Table 1. The angular width of regions Δ (107), (109), around the geometrical boundaries, inside which for given parameters $k\varrho$ and $k\varrho_0$ expression (79) is invalid, and the distances ϱ, ϱ_0 for two frequencies f

$k\varrho$	$k\varrho_0$	Δ [°]	ϱ [m]	ϱ_0 [m]	ϱ [m]	ϱ_0 [m]
			$f = 500$ [Hz]	$f = 500$ [Hz]	$f = 1000$ [Hz]	$f = 1000$ [Hz]
1000	∞*	8	100	∞	50	∞
1000	1000	3	100	100	50	50
500	∞	11	50	∞	25	
500	1000	14	50	100	25	50
500	500	15	50	50	25	25
250	∞	15	25	∞	12.5	∞
250	1000	17	25	100	12.5	50
250	500	19	25	50	12.5	25
250	250	22	25	25	12.5	12.5
125	∞	22	12.5	∞	6.3	∞
50	∞	34	5	∞	2.5	∞
25	∞	50	2.5	∞	1.3	∞
10	∞	84	1	∞	0.5	∞

* denotes a plane wave

3. Efficiency of the half-plane and wedge as obstacles disturbing the acoustic field

Comparative analysis of the interaction between the three chosen wave types and a half-plane and a wedge can be carried on only for the systems in which the source and the observation point are far from the diffraction edges. Exactly, such situations are met in urban systems. In these systems, if the observation point is far enough (75) from the geometrical boundaries, the diffraction part of the acoustic potential can be determined for a half-plane from expression (79), for a wedge from expression (86).

Knowing the geometrical parts of potentials (5), (19) and the diffraction parts (10), (24), it is possible to determine the acoustic field on the geometrical boundaries. The diffraction wave related to the vanishing geometrical wave takes the value according to (47). For the wedge, the diffraction wave having directional coefficient with a singularity takes the value according to (93). The other diffraction waves, which are not related to the disappearing geometrical wave, can be determined according to (79) if condition (75) is satisfied.

If the widths Δ of the regions around the geometrical boundaries (Table 1) are not too large, in keeping with the principle of continuity of the acoustic field, extrapolation can be carried out between the value of the acoustic potential on the geometrical boundary and the last of the values calculated according to the

approximation conditions. In this way, a description of the field throughout the region around the obstacle is obtained. To determine quantitatively the disturbance caused in the free field by the presence of a half-plane or a wedge, the obstacle efficiency is introduced:

$$IL = -20\log\frac{|V|}{|V^i|}, \tag{111}$$

where V is the total acoustic potential of the field disturbed by the obstacle and V^i is the acoustic potential of the free field (of the incident wave). With such a definition of the efficiency of an obstacle, the fact that it takes positive values at the observation point means a decrease in the sound pressure level caused by the presence of the obstacle; the fact that it takes negative values represents an increase in the sound pressure level caused by the presence of the obstacle.

The obstacle efficiency in the case of a half-plane ($\nu = 2$) and a wedge ($\nu = 3/2$), regarded as ideally rigid, is a function of the position of the observation point (ϕ, k_0, z) and that of the source (ϕ_0, k_0, z_0) with respect to the diffraction edge,

$$IL = IL(\phi, \phi_0, k\varrho, k\varrho_0, z, z_0, \nu). \tag{112}$$

It follows from the considerations in subsection 1.2 that the dependence of the obstacle efficiency on particular parameters can be determined analytically only in the shadow area:

$$\phi_{GC} < \phi < \nu\pi. \tag{113}$$

In this area, the acoustic potential contains only the diffraction part which can be represented in the form of one diffraction wave (79) for the half-plane, (86) for the wedge, related to the phase and amplitude of the incident wave ($V^i(R)$).

In the regions where there is interference between geometrical and diffraction waves only numerical analyse is possible. The efficiency is calculated as a function of one parameter with the other fixed.

3.1. Efficiency of the half-plane and wedge in the shadow area

The shadow area occurs at the same time in the case of both obstacles a half-plane ($\nu = 2$) and a wedge ($\nu = 3/2$) if the source is situated in the angular interval $(0, \pi/2)$ (Fig. 5 (II)). Then, the obstacle efficiency according to (79) and (86) has the form

$$IL = 20\log\frac{\sqrt{2\pi k\varrho}}{|P(\phi, \phi_0, \nu)|} - 20\log[d(R)]. \tag{114}$$

Taking into acount expressions (81)–(83), the obstacle efficiency for the three chosen wave types can be given by:

– for a plane wave

$$IL_p = 10\log(2\pi k\varrho) - 20\log|P(\phi, \phi_0, \nu)|, \tag{115}$$

– for a cylindrical wave

$$IL_c = IL_p - 10\log(R/\varrho_0), \tag{116}$$

– for a spherical wave

$$IL_s = IL_p - 10\log(R^2/R_1\varrho_0). \tag{117}$$

It follows from formula (115) that the obstacle efficiency for a plane wave in the shadow area is the greater the farther from the diffraction edge the observation points and the farther it is from the shadow boundary. In the first case the value of the parameter $k\varrho$ defining the relative position of the observation point (calculated in wave lenghts) is large. In the second case the absolute value of the directional coefficient $P(\phi, \phi_0, \nu)$ [5] is small. The fact that the obstacle efficiency in the shadow area for cylindrical and spherical waves is greater or smaller than the efficiency for a plane wave depends on whether the quotients in the second terms of formulae (116) and (117) are greater or smaller than unity. Moreover, for each of the three wave types the inequality occurs:

$$IL_j(\phi, \phi_0, k\varrho, k\varrho_0, k|z-z_0|, \nu = 2) - IL_j(\phi, \phi_0, k\varrho, k\varrho_0, k|z-z_0|, \nu = 3/2) > 0, \quad j = p, c, s, \tag{118}$$

meaning that for the same positions of the source and the observation point the efficiency of a half-plane in the shadow area is always greater than that of a right angle wedge. At the same time, the shadow area for the half-plane is always greater than that for the wedge, since part of the shadow area which occurs in the case of the half-plane is occupied by the wedge itself.

3.2. *Numerical examples*

The calculations were made for two types of obstacle, a half-plane ($\nu = 2$) and a right angle wedge ($\nu = 3/2$). Three types of incident waves were assumed: plane, cylindrical and spherical (for $z = z_0$). For cylindrical and spherical waves, a symmetrical system ($k\varrho, k\varrho_0 = 250, 500, 1000$) and nonsymmetrical one ($k\varrho \neq k\varrho_0$) were taken, with $k\varrho$ and $k\varrho_0$ occurring in three combinations of values used in the symmetrical system. Four positions of the source were chosen, belonging to successive regions distinguished in Fig. 5:

$\phi_0 = 10°$ with the source in region I (32),

$\phi_0 = 55°$ with the source in region I (32),

$\phi_0 = 90°$ with the source on the boundary between region I (32) and region II (37),

$\phi_0 = 135°$ with the source in region III (40) and, at the same time, in region IV (43).

Table 2 lists the parameters for which the calculations were made.

The positions of the source in region I:

$$\phi_0 = 10°, 55°$$

Table 2. The values of parameters and wave types for which the obstacle efficiences were calculated

angular source position	obstacle kind	wave type	$k\varrho_0$	$k\varrho$	$k\varrho/k\varrho_0 = m$
$\phi_0 = 10°, 55°,$ $90°, 135°$	$\nu = 2,\ 3/2$	plane	∞	250	0
			∞	500	0
			∞	1000	0
		cylindrical	250	250	1
			500	500	1
			1000	1000	1
			1000	250	1/4
			1000	500	1/2
		spherical	500	250	1/2
			250	250	1
			500	500	1
			1000	1000	1
			1000	250	1/4
			1000	500	1/2
			500	250	1/2

are related to the presence of the shadow area for both of the obstacle. With the position of the source:

$$\phi_0 = 90°,$$

the shadow area occurs only for the half-plane and it disappears for the wedge. The position of the source:

$$\phi_0 = 135°$$

causes the appearance of the shadow for the half-plane. In the case of the wedge, there is no shadow, on the other hand, there is a wave reflected from the half-plane $\phi = 3\pi/2 = 270°$. Table 3 shows the appropriate geometrical boundaries ϕ_{GC}, ϕ_{GD}, $\phi_{GD'}$, and in view of this, it is possible to distinguish four areas (Fig. 6):

– area A:

$$0 < \phi < \phi_{GD} \tag{119}$$

(which always occurs for the numerical examples)

– area B:

$$\phi_{GD} < \phi < \begin{cases} \phi_{GC} & \text{(for all the positions of the source in the case of the half-plane and for the wedge for the source position } \phi_0 = 10°,\ 55°,\ 90°\text{),} \\ \phi_{GD'} & \text{(for the wedge, for } \phi_0 = 135°\text{),} \end{cases} \tag{120}$$

Table 3. The positions of the geometrical boundaries for the numerical examples for the given angular position of the source ϕ_0

ϕ_0 [°]	ν	shadow boundary $\phi_{GC} = \pi + \phi_0$ [°]	boundary of wave reflected from half-plane $\phi = 0$ $\phi_{GD} = \pi - \phi_0$ [°]	boundary of wave reflected from half-plane $\phi = 3\pi/2 = 270°$ $\phi_{GD'} = 2\pi - \phi_0$ [°]
10	2	190	170	–
	3/2	190	170	–
55	2	235	125	–
	3/2	235	125	–
90	2	270	90	–
	3/2	–	90	270
135	2	315	45	–
	3/2	–	45	225

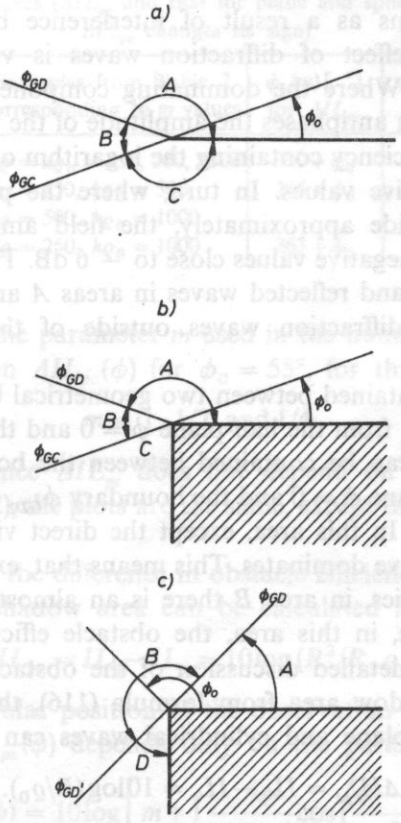

FIG. 6. Areas *A*, *B*, *C*, and *D* around the half-plane (*a*) and around the wedge (*b*), (*c*) distinguished in terms of the character of the function IL (ϕ) describing the efficiency of the obstacle

– area C:

$$\phi_{GC} < \phi < \begin{cases} 360^\circ & \text{(for the half-plane),} \\ 270^\circ & \text{(for the wedge),} \end{cases} \tag{121}$$

– area D (which occurs only for the wedge for $\phi_0 = 135^\circ$)

$$\phi_{GD} < \phi < 270^\circ. \tag{122}$$

In the numerical examples large values of the parameters $k\varrho$ and $k\varrho_0$ describing the relative positions of the observation point and the source we assumed, therefore outside of the direct vicinity of the geometrical boundaries the amplitudes of the diffraction waves are small [5]. This explains the structure of the acoustic fields in the distinguished areas A, B, C and D and the resultant shape of the function $IL(\phi)$ describing the obstacle efficiency in these areas.

Area C – the shadow area – is one where only diffraction waves occur. In this area the obstacle efficiency is positive and increases while deepening into it.

In areas A and D the acoustic field has the same structure since in the areas the direct wave ($V^i(R)$) and one of the reflected waves ($V^i(R')$ or $V^i(R'')$) occur as the dominating component waves.

The total field forms as a result of interference between geometrical and diffraction waves. The effect of diffraction waves is visible only close to the geometrical boundaries. Where the dominating component waves (the direct and reflected ones) interfere in antiphases the amplitude of the total field is close to zero, therefore the obstacle efficiency containing the logarithm of the field amplitude (111) can take the large positive values. In turn, where the phases of the dominating component waves coincide approximately, the field amplitude doubles and the obstacle efficiency takes negative values close to – 6 dB. The latter fact confirms the dominance of the direct and reflected waves in areas A and D, and simultaneously the small influence of diffraction waves outside of the direct vicinity of the geometrical boundaries.

Area B is the one contained between two geometrical boundaries: the boundary ϕ_{GD} of the wave reflected from the half-plane $\phi = 0$ and the shadow boundary ϕ_{GC}. For the wedge, area B can be contained between the boundary ϕ_{GD} of the wave reflected from the half-plane $\phi = 0$ and the boundary $\phi_{GD'}$ of the wave reflected from the half-plane $\phi = 270^\circ$. In this area, except the direct vicinity of the geometrical boundaries, the direct wave dominates. This means that, except the direct vicinity of the geometrical boundaries, in area B there is an almost undisturbed field of the incident wave. Therefore, in this area, the obstacle efficiency is equal to zero.

Passing to a more detailed discussion of the obstacle efficiency in the areas distinguished, in the shadow area from formula (116), the difference between the obstacle efficiencies for plane and cylindrical waves can be calculated:

$$\Delta IL_{pc} = IL_p - IL_c = 10\log(R/\varrho_0). \tag{123}$$

For a given angular position of the source (ϕ_0) the difference between the obstacle

efficiencies for plane and cylindrical waves, as a function of the angular position of the observation point (ϕ), depends only on the parameter

$$m = k\varrho/k\varrho_0, \tag{124}$$

then

$$\Delta IL_{pc}(\phi) = 5\log[1+m^2-2m\cos(\phi-\phi_0)]. \tag{125}$$

As a function of the angle ϕ, $\Delta IL_{pc}(\phi)$ is at first positive, then deeper into the shadow area it takes negative values. This means that deeper into the shadow the obstacle efficiency for cylindrical wave becomes greater than that for a plane wave:

$$\begin{aligned} &\Delta IL_{pc}(\phi) > 0 \quad \text{for} \quad \phi_{GC} < \phi < \phi_k(m), \\ &\Delta IL_{pc}(\phi) < 0 \quad \text{for} \quad \phi > \phi_k(m). \end{aligned} \tag{126}$$

Table 4 gives the approximate values of the angles $\phi_k(m)$ for which ΔIL_{pc} changes its

Table 4. The values of the angles $\phi_k(m)$ for which in the shadow area the difference between the obstacle efficiency for plane and cylindrical waves (ΔIL_{pc} and that for plane and spherical waves ΔIL_{ps} changes its sign)

m	Examples from Table 2 corresponding to m values	$\phi_k(m)$[°] for ΔIL_{pc}	$\phi_k(m)$ [°] for ΔIL_{ps}
1	$k\varrho = k\varrho_0 = 250, 500, 1000$	$300+\phi_0$	$270+\phi_0$
1/2	$k\varrho = 250$, $k\varrho_0 = 500$ $k\varrho = 500$, $k\varrho_0 = 1000$	$285+\phi_0$	$254+\phi_0$
1/4	$k\varrho = 250$, $k\varrho_0 = 1000$	$263+\phi_0$	$248+\phi_0$

sign, for three values of the parameter m used in the numerical examples (Table 2). The plots of the function $\Delta IL_{pc}(\phi)$ for $\phi_0 = 55°$, for three values of m:

$$m = 1,\ 1/2 \text{ and } 1/4,$$

are shown in Fig. 7. Since ΔIL_{pc} does not depend on ν for the two obstacles considered ($\nu = 2$, $\nu = 3/2$), the plots are the same, except that for the wedge they end for $\phi = 270°$.

From formula (117), the difference in obstacle efficiency between the plane and spherical waves in the shadow area can be calculated from the formula

$$\Delta IL_{ps} = IL_p - IL_s = 10\log(R^2/R_1\varrho_0). \tag{127}$$

As a function of the angular position of the observation point ϕ, for $z = 20$, with given values of ϕ_0, $\Delta IL_{ps}(\phi)$ depends only on the parameter m:

$$\Delta IL_{ps}(\phi) = 10\log\left[m+1-\frac{4m}{m+1}\cos\left(\frac{\phi-\phi_0}{2}\right)^2\right]. \tag{128}$$

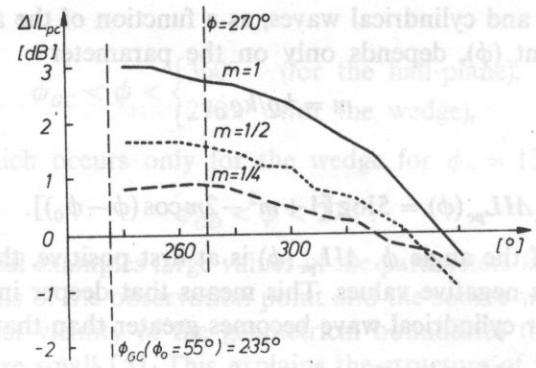

FIG. 7. The difference $\Delta IL_{pc}(\phi)$ 125 between the obstacle efficiencies for plane and cylindrical waves for different values of the parameter $m = 1,\ 1/2$ and $1/4$

The difference in the obstacle efficiency between the plane and spherical waves in the shadow area changes its sign for the angles $\phi_k(m)$ (Table 4):

$$\begin{aligned} \Delta IL_{ps}(\phi) &> 0 \quad \text{for} \quad \phi_{GC} < \phi < \phi_k(m), \\ \Delta IL_{ps}(\phi) &< 0 \quad \text{for} \quad \phi > \phi_k(m). \end{aligned} \tag{129}$$

The plots of $\Delta IL_{pk}(\phi)$ for $\phi_0 = 55°$ are shown in Fig. 8.

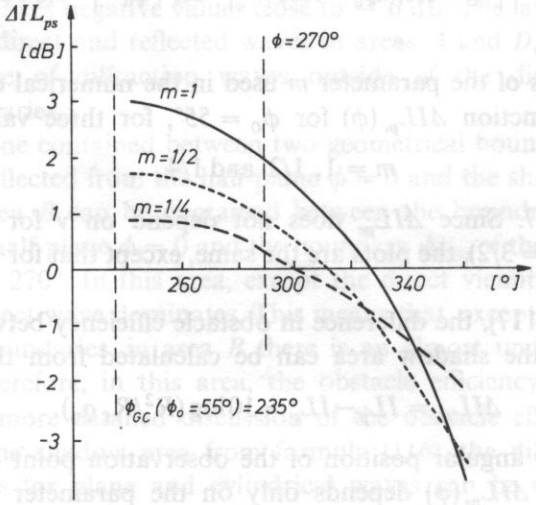

FIG. 8. The difference $\Delta IL_{ps}(\phi)$ (128) between the obstacle efficiencies for plane and spherical waves for different values of the parameter $m = 1,\ 1/2$ and $1/4$

From formula (118) the efficiency of the half-plane in the shadow area is always greater than that of the right angle wedge:

$$\Delta IL_v = IL(v=2) - IL(v=3/2) = 20\log\left[\frac{|P(\phi,\phi_0,v=3/2)|}{|P(\phi,\phi_0,v=2)|}\right] > 0. \qquad (130)$$

The plot of difference (130) as a function of the angular position of the observation point ϕ for $\phi_0 = 10°$, 55°, is shown in Fig. 9.

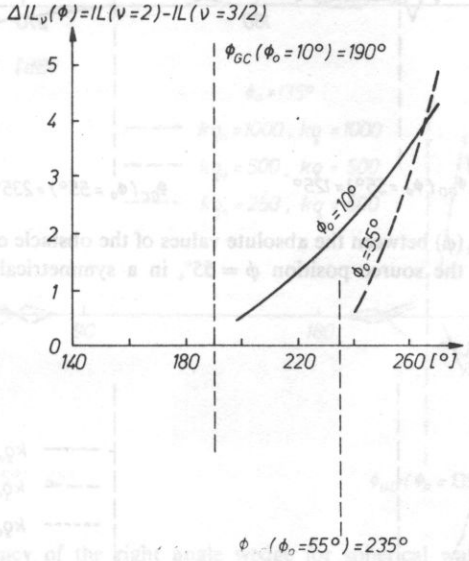

FIG. 9. The difference $\Delta IL(\phi)$ (130) between the efficiencies of the half-plane and the right angle wedge in the shadow area for two source positions $\phi_0 = 10°$, 55°

Analyzing the obstacle efficiencies in areas A and D for the chosen range of parameters (Table 2), it can be said that for a given wave type, the same position of the source (ϕ_0, $k\varrho_0$) and the observation point (ϕ, $k\varrho$) the efficiency of the half-plane and the right angle wedge does not show differences with an accuracy up to hundreths of a decibel:

$$IL_j(v=2) \cong IL_j(v=3/2), \quad j = p,c,s. \qquad (131)$$

It follows from comparison of the efficiency for the cylindrical wave IL_c and that of the spherical wave IL_s in areas A and D, that for the same positions of the source and the observation point the positions of the maxima and minima of the efficiency are the same. On the other hand the absolute values of the efficiency $|IL_c|$ for the cylindrical wave are almost always greater than those of the efficiency $|IL_s|$ for the spherical wave:

$$\Delta|IL|_{cs} = |IL_c| - |IL_s| > 0. \qquad (132)$$

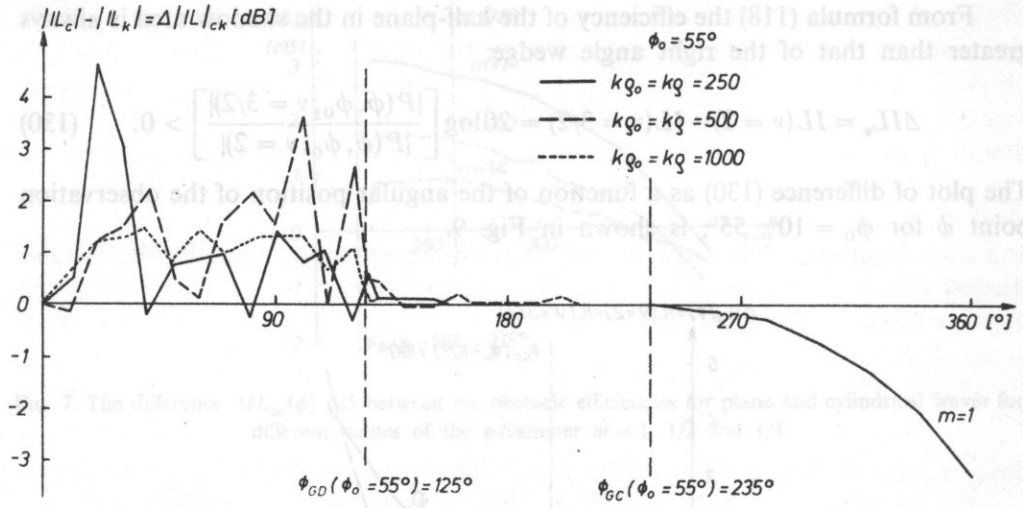

FIG. 10. The difference $\Delta|IL|_{ck}(\phi)$ between the absolute values of the obstacle efficiency for cylindrical and spherical waves for the source position $\phi = 55°$, in a symmetrical system $kq = kq_0$

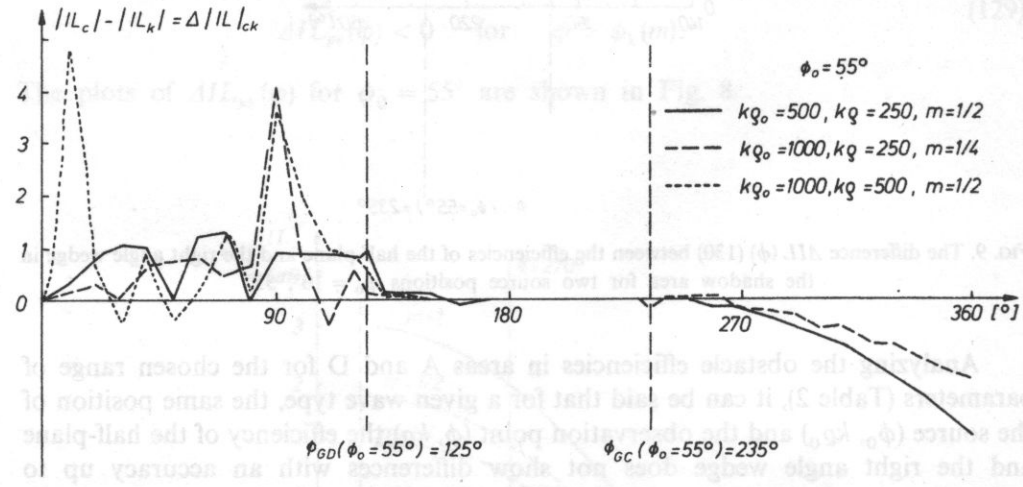

FIG. 11. The difference $\Delta|IL|_{ck}(\phi)$ between the absolute values of the obstacle efficiency for cylindrical and spherical waves for the source position $\phi_0 = 55°$, in a nonsymmetrical system $kq \neq kq_0$

This is shown in Figs. 10 and 11 for symmetrical and nonsymmetrical positions of the source and the observation point with respect to the diffraction edge, for $\phi_0 = 55°$. The fact that for the cylindrical wave in areas A and D the absolute values of the efficiency $|IL_c|$ are greater than those of $|IL_s|$ for the spherical wave, can be explained by the existence of a greater degree of spatial correlation between the dominating component waves which form the field in the case of a cylindrical wave.

For the numerical examples, area D, where the dominating components are the direct wave ($V^i(R)$) and the geometrical wave reflected from the half-plane $\phi = 270°$ ($V^i(R'')$) occurs for $\phi_0 = 135°$, i.e., for the position of the source on the axis of symmetry of the wedge. Hence, the acoustic fields, and, thus, the efficiencies, in areas D and A are the same (see Fig. 12). For comparison, Fig. 13 shows the efficiency of the half-plane for $\phi_0 = 135°$. It can be seen from these figures that the efficiencies of the half-plane and the wedge in area A are the same. Moreover, it can be seen that in the case of the half-plane, area D does not occur, and is replaced by the shadow area C.

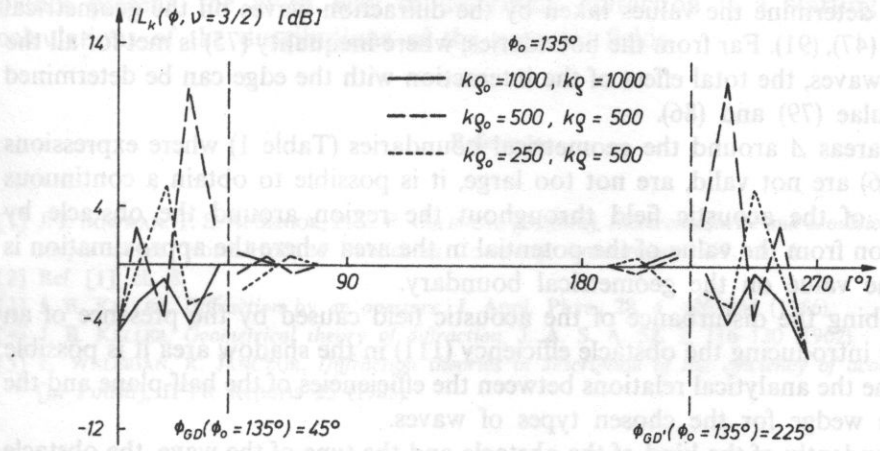

FIG. 12. The efficiency of the right angle wedge for spherical waves for $\phi_0 = 135°$

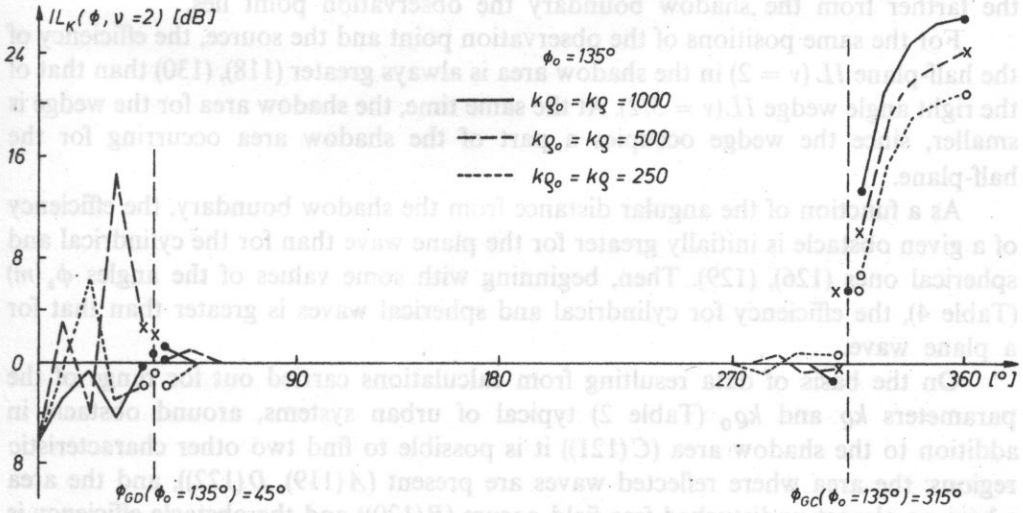

FIG. 13. The efficiency of the half-plane for spherical waves for $\phi_0 = 135°$

4. Conclusion

For the presented six cases of interaction between successively plane, cylindrical and spherical waves, and the edges of an ideal rigid half-plane and an ideal rigid wedge a uniform description of the acoustic field structure is achieved. It consists of the geometrical part (5), (19) and the diffraction part (10), (24) of the acoustic potential. It applies to systems in which, from conditions (58), (62) and (63), both the source and the observation point are far from the diffraction edge.

In the diffraction part of the potential, diffraction waves defined by formulae (73) and (74) and tied up to the appropriate geometrical waves were found. This made it possible to determine the values taken by the diffraction waves on the geometrical boundaries (47), (91). Far from the boundaries, where inequality (75) is met for all the diffraction waves, the total effect of the interaction with the edge can be determined from formulae (79) and (86).

If the areas Δ around the geometrical boundaries (Table 1) where expressions (79) and (86) are not valid, are not too large, it is possible to obtain a continuous description of the acoustic field throughout the region around the obstacle by extrapolation from the value of the potential in the area where the approximation is valid to the value on the geometrical boundary.

Describing the disturbance of the acoustic field caused by the presence of an obstacle by introducing the obstacle efficiency (111) in the shadow area it is possible to determine the analytical relations between the efficiencies of the half-plane and the right angle wedge for the chosen types of waves.

Independently of the kind of the obstacle and the type of the wave, the obstacle efficiency IL in the shadow area (114) is the greater the farther from the diffraction edge the observation point and the source are, and the deeper into the shadow area the farther from the shadow boundary the observation point lies.

For the same positions of the observation point and the source, the efficiency of the half-plane $IL(\nu = 2)$ in the shadow area is always greater (118), (130) than that of the right angle wedge $IL(\nu = 3/2)$. At the same time, the shadow area for the wedge is smaller, since the wedge occupies a part of the shadow area occurring for the half-plane.

As a function of the angular distance from the shadow boundary, the efficiency of a given obstacle is initially greater for the plane wave than for the cylindrical and spherical ones (126), (129). Then, beginning with some values of the angles $\phi_k(m)$ (Table 4), the efficiency for cylindrical and spherical waves is greater than that for a plane wave.

On the basis of data resulting from calculations carried out for range of the parameters $k\varrho$ and $k\varrho_0$ (Table 2) typical of urban systems, around obstacle in addition to the shadow area (C(121)) it is possible to find two other characteristic regions: the area where reflected waves are present (A(119), D(122)), and the area where an almost undisturbed free field occurs (B(120)) and the obstacle efficiency is zero.

In areas where reflected waves occur (A, D) the obstacle efficiency can take large values at points where the dominating component waves (direct and reflected) interfere in antiphases. At points where they interfere in the same phases, the barrier efficiency takes negative values of about -6 dB.

The comparative analysis performed makes it possible to draw conclusions about the structure of the acoustic fields around the obstacle in question. In real urban system where the dominating phenomenon forming the acoustic field, is the diffraction at an edge, or a right angle wedge, from the formulae here it is possible to determine the obstacle efficiency in regions where the approximation conditions are satisfied. In areas for which it is necessary to consider interaction with additional planes present, the given way of describing diffraction is a starting point for calculations of the distributions of the acoustic fields.

References

[1] J. J. BOWMAN, T. B. A. SENIOR, P. L. E. USLENGHI [editors], *Electromagnetic and acoustic scattering by simple shapes*, North-Holland Publishing Company, Amsterdam 1969, ch. 6.
[2] Ref. [1], ch. 8.
[3] J. B. KELLER, *Diffraction by an aperture*, J. Appl. Phys., **28**, 4, 426–444 (1956).
[4] J. B. KELLER, *Geometrical theory of diffraction*, J. A. S. A. **52**, 2, 116–130 (1962).
[5] E. WALERIAN, R. JANCZUR, *Diffraction theories in description of the efficiency of acoustic sciences* [in Polish], IFTR Reports 25 (1985).

Received February 25, 1987.